JOURNAL OF MATERIALS SCIENCE 27 (1992) 6673–6678

Influence of slip-casting and dry-pressing on structure evolution of alumina compacts

H. H.-D. LEE
Metallurgy Department, General Motors Research Laboratories, Warren, MI 48090, USA

A commercial alumina powder was processed to remove aggregates and agglomerates for the study of processing influence on sintering behaviour and structure evolution. Slip-casting a uniformly dispersed slurry formed green compacts with homogeneous particle packing, which subsequently resulted in a nearly defect-free microstructure upon sintering. Dry-pressing the granules that possessed a similar homogeneous microstructure led to compacts with larger voids and particle-packing inhomogeneity. The inhomogeneity persisted through sintering and evolved voids with a size of about 6 μm. However, under the same sintering condition, the sintered density of the dry-pressed compact approached that of the slip-cast compact. The grain sizes of both sintered compacts were similar, implying that differences in consolidation effectiveness do not necessarily incur variation in grain growth provided the compacts are prepared from the same starting powder and sintered under the same condition.

1. Introduction

In the consolidation of ceramic powders, it is generally known that slip-casting is superior to dry-pressing for forming components with better structures. This is due mainly to the lack of powder fluidity in the operation of dry pressing, resulting in inhomogeneous particle-packing structures. While the influence of particle packing on structure evolution has been extensively investigated, many studies [1–6] are actually based on the sintering of as-received commercial powders. Unfortunately, the as-received powders often contain aggregates and agglomerates in which primary particles are bound in face-to-face and edge-to-edge contact, respectively [7–10]. These structures may differ greatly from the surrounding particles, leading to a substantial variation in structure evolution upon sintering. Therefore, the interpretation of the sintering results obtained from dry-pressing the as-received commercial powders may become intangible. For example, it is rather difficult to ascribe distinctly the observed sintering inhomogeneity and densification incompleteness [11–15] to either powder aggregates/agglomerates or the consolidation ineffectiveness of dry-pressing.

There are several studies [16–19] showing that the use of non-aggregated and non-agglomerated powders in slip-casting can lead to improved microstructures, but none of these studies used powders with identical characteristics for the evaluation of the consolidation effectiveness between slip-casting and dry-pressing. Furthermore, most slurries used in slip-casting have been prepared by pH adjustment [16–18] while the granules [2, 20] used in dry-pressing often contain binders. Under the circumstances, a substantial difference in particle packing has already pre-existed between the starting powders and the granules prior to the processing of consolidation. In addition, the involvement of binders may introduce impurities and affect subsequent sintering behaviour. For these reasons, the influence of consolidation effectiveness on structure evolution cannot be directly derived from a simple comparison of the existing results shown in the literature.

In this study, accordingly, a commercial alumina powder was first processed to remove aggregates and agglomerates. Then, the processed powder was slip-cast to form green compacts with a uniform structure. After drying, a portion of the green compacts was ground to form small granules which retained the uniform structure originating from the process of slip-casting. These granules were dry-pressed to form compacts for a study of structure evolution. Because these granules have a basic structure similar to that of the slip-cast compacts, the obtained differences in structure evolution are thus the direct consequence of particle-rearranging variation during consolidation. The results are discussed with respect to particle-packing morphology, distribution of particle-packing channels, green and sintered densities, and sintered microstructure.

2. Experimental procedure

2.1. Powder and compact preparation

Water with a pH of $\simeq 3$ was used in order to raise sufficient electrostatic repulsive forces among particles for the suspension of a commercial α-alumina powder. The suspension was allowed to stand under gravity for the settling of aggregates and agglomerates. As a result of this sedimentation, a powder with a narrower size distribution was obtained.

0022–2461

The processed powder was used to form a 55 vol% slurry for slip-casting. A portion of the slip-cast compact was dried in an oven and then ground with a mortar and pestle to form small granules. After grinding, granules larger than 125 μm diameter were screened out with a US standard 115-mesh sieve. The sized granules were dry-pressed at a pressure of 34 MPa in a stainless steel die lightly lubricated with oleic acid. Both slip-cast and dry-pressed compacts were sintered in air to 1520°C in a dilatometer (thermal dilatometer analyser, Model TD-726, and thermal analysis control system, (model Cyber-701), Harrop Industries, OH). The heating rate was 5°C min^{-1}, and the soaking time at 1520°C was 1 h.

2.2 Powder and compact characterization

The microstructures of particles (including aggregates/agglomerates and primary particles) were examined using scanning electron microscopy (SEM). Particle size was monitored by a particle size analyser (Autosizer II, Malvern Instruments, UK) utilizing the principle of the intensity fluctuation technique. The observed weight-average mean particle size was further correlated with the surface-area equivalent spherical diameters derived from three-point BET measurements (Model CS-5, Quantachrome Corporation, NY).

Green compact density (or particle-packing density) was determined from the weight and dimensions of the dry samples, which had a minimal weight of 80 g. The densities of sintered compacts were determined using a hydrostatic weighing method. A theoretical density of 3.98 g cm^{-3} was used to calculate the relative density of the sintered compacts. To find if pores were open, sintered samples were immersed in water while being degassed under a 0.1 MPa vacuum for 20 min, then the samples were weighed again.

The particle-packing characteristics of the dry-pressed compacts and the slip-cast compacts were studied by mercury porosimetry (Poresizer 9310, Micrometrics, GA). Because the green compacts were fragile and could be shattered during handling, the samples were bisqued (i.e. presintered) by heating to 440°C at a rate of 0.5°C min^{-1} and then to 1000°C at a rate of 1°C min^{-1}. The temperature of 1000°C was held for 1 h. Then, the compacts were dry polished using 600-grit polishing paper and blown free of debris by compressed air. This allows the characterization of interior pore/particle-packing structure. The sizes of the samples were limited to 1 cm^3, in order for the mercury in the capillary of the porosimeter to be adequate to fill up the porosity of the sample. The intrusion pressure ranged from 0.02–89 MPa, corresponding to pore diameters of 58–0.014 μm. The distribution of particle-packing channels was calculated using a mercury surface tension of 0.485 Nm^{-1} and a contact angle of 130°. Average pore diameter is calculated from the equation of $4V/A$, where V is the pore volume and A is the pore area, by assuming that all pores are right cylinders.

The microstructures of the fractured and fractured-and-polished surfaces of the sintered compacts were examined using SEM. The polishing of the fractured surfaces included the use of 600-grit polishing paper and 1 μm diamond paste. Then, the polished samples were thermally etched at 1300°C for 10 h to reveal grain boundaries. Average grain sizes were determined from the scanning electron micrographs, using the linear intercept technique [21].

3. Results and discussion

3.1 Characterization of powders and green microstructure

The as-received powder contained hard aggregates and agglomerates made of primary particles, as shown in Fig. 1a and b, respectively. Both aggregates and agglomerates were completely removed by sedimentation, leading to a powder with a particle size distribution as displayed in Fig. 2. The weight average mean particle size of 0.26 μm obtained from the particle size analyser was close to the surface-area equivalent spherical diameter of 0.21 μm derived from the measured BET value of 7.2 $m^2 g^{-1}$. Thus, the particles were dispersed in primary particle form.

Slip-casting the well-dispersed particles formed green compacts with a uniform and dense particle-packing structure. As seen in Fig. 3a, the surface of the slip-cast compact had no packing imperfections larger than mean particle size. In the interior of the slip-cast

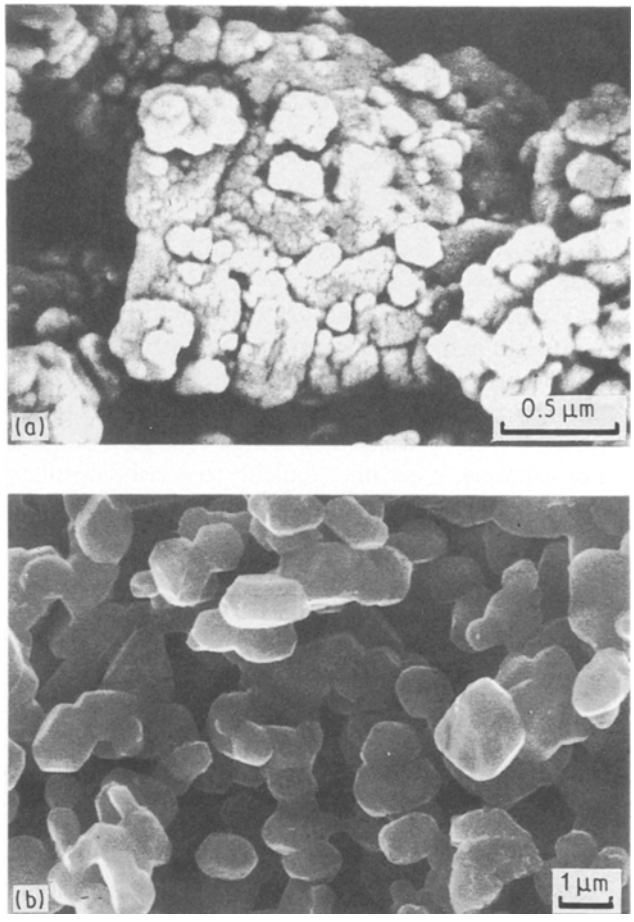

Figure 1 Scanning electron micrographs of (a) aggregates and (b) agglomerates in the as-received alumina powder.

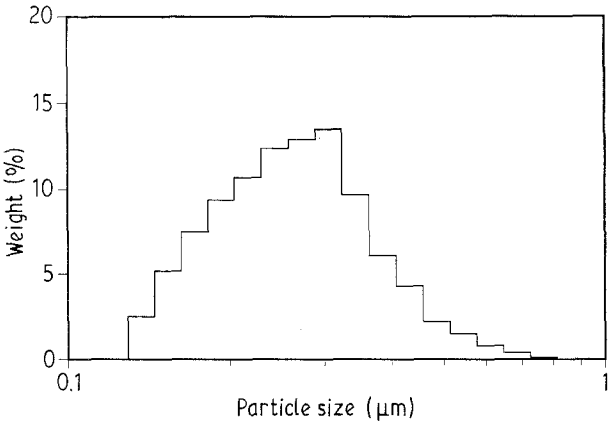

Figure 2 Particle size distribution of the processed powder.

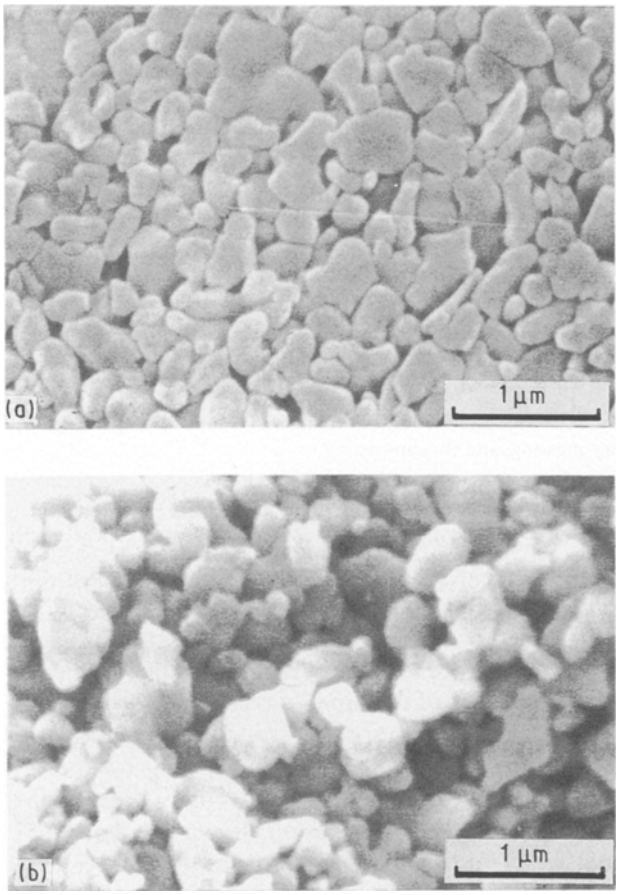

Figure 3 Uniform and dense particle packing in the slip-cast compact: (a) top surface and (b) interior.

compact, the particles were also densely and uniformly packed, Fig. 3b. Possessing this type of surface and bulk packing structure, a slip-cast compact reached a packing density of 69.4%. For dense random packing of equal spheres, numerical models have predicted 57%–62% theoretical density [22–26] and the generally accepted upper limit is 64% [25, 27, 28]. The high packing density of 69.4% in the present sample, therefore, demonstrates that the irregular-shaped particles are homogeneously and densely consolidated throughout the entire compact.

The particle assembly on the as-pressed surface was loose and non-uniform as compared with that of slip-cast compacts. The interior particle packing of the dry-pressed compact varied from a uniform and dense particle-packing structure to a bridge-type structure. The dense area had a particle-packing structure resembling its preceding microstructure as shown in Fig. 3b. But, holes or packing imperfections as large as 1 μm across were seen in the loosely packed area of Fig. 4. Apparently, in the dry state, the rearrangement of particles toward a uniform structure was restricted even under a substantial external force. Understandably, the packing densities of the dry-pressed compacts were low and varied from 56%–60%.

Fig. 5 displays the distributions of particle-packing channels for the slip-cast and the dry-pressed compacts, with packing densities of 69% and 59%, respectively. The slip-cast compact had a narrow distribution ranging from 0.02–0.08 μm, and an average pore diameter of 0.067 μm. The ratio of the most frequently detected particle-packing channel diameter (0.07 μm) to the most frequently detected particle size (0.30 μm seen in Fig. 2) is 0.23.

Unlike the slip-cast compact, in this study, the dry-pressed compact had a particle-packing distribution spreading bimodally from 0.02–0.12 μm. The main peak located at 0.1 μm, and the minor peak appeared at 0.07 μm as a shoulder to the main peak. The latter value is identical to the most frequently detected particle-packing channel diameter obtained for the slip-cast compact. This indicates the fact that a portion of the dry-pressed compact retained the dense

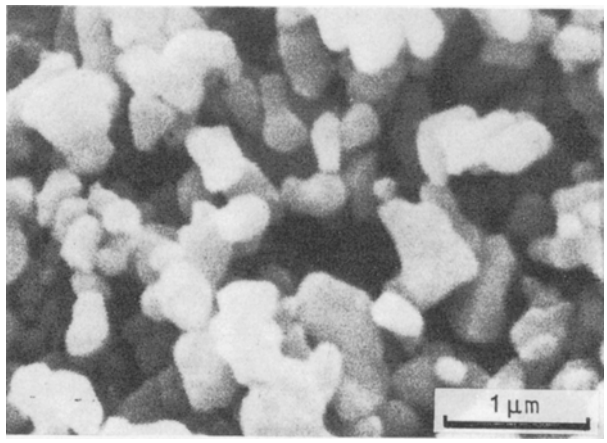

Figure 4 Scanning electron micrograph showing a loosely packed microstructure for the dry-pressed compact.

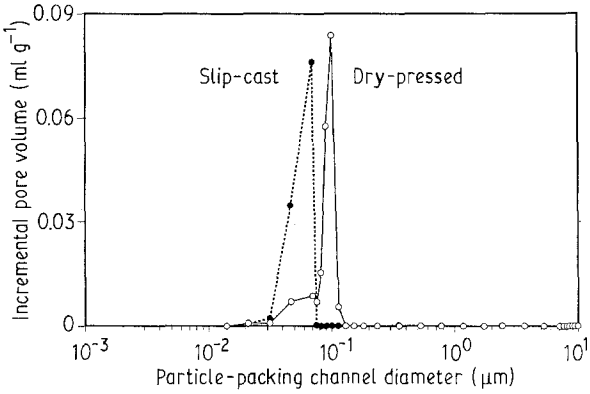

Figure 5 Distributions of particle-packing channel diameters for the slip-cast compact and the dry-pressed compact.

particle-packing structure originating from the slip-casting operation. However, its fraction is only about 20%. Furthermore, in this dry-pressed compact, no local area had particle-packing channels smaller than those of the slip-cast compact. Instead, particle-packing channels larger than 0.08 μm were formed. This clearly indicates that under this external force, dry-pressing cannot consolidate the granules into a structure denser than that obtained from slip-casting.

The main peak of this dry-pressed compact can be considered as the particle-packing channels of the inter-granules. In this case, the ratio of the most frequently detected particle-packing channel diameter (0.1 μm) to the most frequently detected particle size (0.30 μm) is 0.33, which is much higher than the value of 0.23 calculated for the slip-cast compact. This further confirms the difficulty of particle rearrangement toward a dense and uniform structure for dry-pressing.

3.2. Sintering behaviour and sintered microstructures

Sintering-induced densification is shown in Fig. 6. The difference in relative density between the slip-cast and the dry-pressed green compacts was 10%, but decreased gradually to 4% upon sintering as the temperature reached 1520° C. Soaking for 1 h at 1520° C increased density to 3.967 and 3.956 g cm^{-3} for the slip-cast and the dry-pressed compacts, respectively. Both compacts did not show any detectable level of water intrusion, indicating that pores in the samples were not interconnected.

The grains on the as-fractured surfaces of both sintered compacts were similar in size, as shown in Fig. 7a and b. In addition, both intergranular and transgranular fracture mechanisms co-existed on the as-fractured surfaces of both sintered compacts. However, after the samples were polished and thermally etched, pores as large as 6 μm diameter were identified for the sintered dry-pressed compacts, Fig. 8a. For the sintered slip-cast compact, Fig. 8b, the number of pores was less and the pore size was considerably smaller than the grain size. Therefore, packing inhomogeneity resulting from improper powder consolidation persists through the final sintering stage.

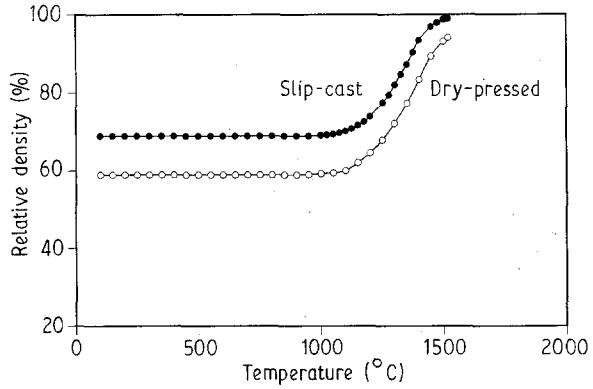

Figure 6 Effect of temperature on densification for the dry-pressed compact and the slip-cast compact.

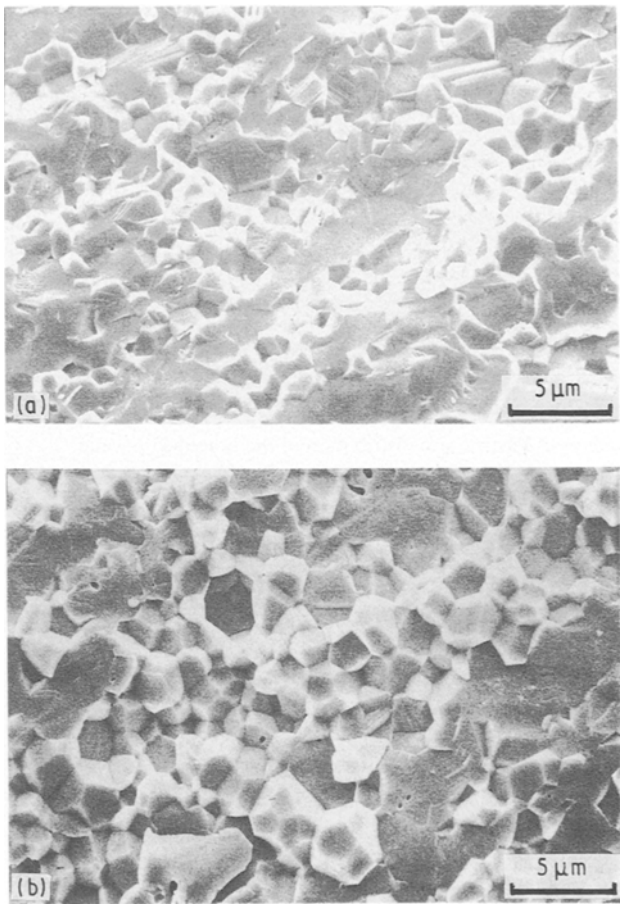

Figure 7 Fracture surfaces of the sintered compacts prepared by (a) dry-pressing, and (b) slip-casting.

The average grain sizes calculated according to the Fullman intercept technique were about 2 μm for both compacts. The sizes of the grains even nearby the large pores seen in Fig. 8a range from 0.5–3 μm, which are similar to those of the slip-cast compact shown in Fig. 8b. The similarity in grain structure indicates that differences in consolidation technique do not necessarily affect grain growth. This observation is inconsistent with the conclusion drawn by Wang [5] that larger grains were obtained for the denser dry-pressed compacts. However, it agrees with the observation reported by Bruch [1] that the rate of grain growth was independent of green density (in the range 22.4%–53.8%). Three reasons may be ascribed to the green density independence of grain growth observed in the present study. First, both green compacts comprised the same starting powder. Secondly, the granules used in the dry-pressing had a basic particle-packing structure similar to that of the slip-cast compact. Thirdly, the green density (59%) of the dry-pressed compact may be high enough to prevent differential grain growth from occurring.

The conclusion mentioned earlier should not be confused with the other well-known phenomenon that at constant sintered density, the green compact with lower packing density or larger pores will evolve a microstructure with larger grain size. This is because a higher sintering temperature is necessary in order for the loosely packed compact to reach the same sintered

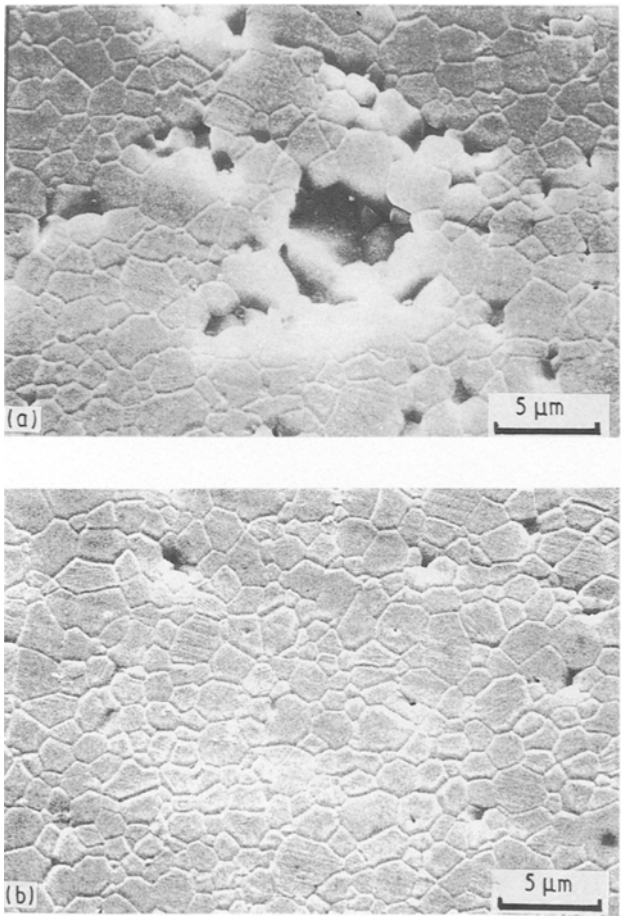

Figure 8 Polished-and-thermally-etched fracture surfaces of sintered compacts prepared by (a) dry-pressing, and (b) slip-casting.

density achieved by the densely packed compact. Under the circumstances, the increase of grain growth is conceivably due to high sintering temperature, instead of low green density. This type of phenomenon is not seen in the present study because grain growth of both compacts is evaluated at the same sintering temperature.

In view of these facts, it is logical to conclude that differences in consolidation technique do not necessarily affect grain growth.

4. Conclusion

A commercial α-alumina powder was processed to remove aggregates and agglomerates before being consolidated to form green compacts by slip-casting. A portion of the slip-cast compact was ground to form granules that retained the uniform structure originating from the process of slip-casting. These compacts were sintered and their microstructure evolution and sintering behaviour were then studied.

Slip-casting a homogeneous slurry formed green compacts with a uniform and dense microstructure. This type of green compact had a density in the vicinity of 69%. Most important, its particle packing approached an ideal close-packed structure. The slip-cast compact sintered to a 99.7% dense and homogeneous microstructure, at a temperature of 1520°C and 1 h soaking. Dry-pressing did not consolidate granules into a compact with structures denser than that inherited from slip-casting. As expected, larger voids and particle-packing channels were introduced to the green compacts, forming a broader distribution of pore structure. The packing densities of the dry-pressed compacts were thus lower and varied from 56% –60%. A dry-pressed compact with green density of 59% sintered to 99.3% under the same sintering condition, but voids with a size of about 6 μm existed. This indicates that particle-packing inhomogeneity can persist through sintering. All these facts reflect that the applied external force cannot overcome the difficulty of particle rearrangements in a dry state.

However, differences in consolidation effectiveness between slip-casting and dry-pressing did not affect grain growth. The green density independence of grain growth (at constant sintering temperature) is a combined consequence of (1) the same starting powder, (2) a similarity in the characteristics of starting powders or granules used in the operation of slip-casting and dry-pressing, and (3) the relatively high packing density of the dry-pressed compact.

Acknowledgements

The author thanks B. Powell and S. Browne for reviewing this paper.

References

1. C. A. BRUCH, *Amer. Ceram. Soc. Bull.* **41** (1962) 799.
2. J. ZHENG and J. S. REED, *J. Amer. Ceram. Soc.* **72** (1989) 810.
3. C. P. CAMERON and R. RAJ, *ibid.* **71** (1988) 1031.
4. *Idem, ibid.* **73** (1990) 2032.
5. D. N. K. WANG, PhD thesis, University of California, Berkley, CA (1976).
6. M. A. OCCHIONERO and J. W. HALLORAN, in 'Sintering and Heterogeneous Catalysis', edited by G. C. Kuczynski, A. E. Miller and G. A. Sargent (Plenum Press, New York, 1984) p. 89.
7. B. HONIGMANN and J. STABENOW, VI FATIPEC Congress (1962) p. 89.
8. B. HONIGMANN, *Ber. Bunsenges. Phys. Chem.* **71** (1967) 239.
9. J. STABENOW, *ibid.* **72** (1968) 374.
10. S. G. LAWRENCE, in "Dispersion of Powders in Liquids with Special Reference to Pigments", 3rd Edn, edited by G. D. Parfitt (Applied Science, London; New Jersey, 1981) p.363.
11. F. W. DYNYS and J. W. HALLORAN, *J. Amer. Ceram. Soc.* **66** (1983) 655.
12. *Idem, ibid.* **67** (1984) 596.
13. W. H. RHODES, *ibid* 64 (1981) 19.
14. J. W. HALLORAN, in "Advances In Ceramics: Forming of Ceramics", Vol. 9, edited by J. A. Mangles and G. L. Messing (The American Ceramic Society, 1984) p.67.
15. G. C. CULBERTSON and J. P. MATHERS, in "Processing of Metal and Ceramic Powders", edited by R. M. German and K. W. Lay (The Metallurgical Society of AIME, Warrendale, PA, 1981) p.109.
16. A. ROOSEN and H. K. BOWEN, *J. Amer. Ceram. Soc.* **71** (1988) 970.
17. E. A. BARRINGER, N. JUBB, B. FEGLEY, R. L. POBER and H. K. BOWEN, in "Ultrastructure Processing of Ceramics, Glasses, and Composites", edited by L. L. Hench and D. R. Ulrich (Wiley, New York, 1984) pp. 315–33.
18. T.-S. YEH and M. D. SACKS, *J. Amer. Ceram. Soc.* **71** (1988) 841.
19. I. A. AKSAY, in "Advances in Ceramics", Vol. 9, "Forming of Ceramics", edited by J. A. Mangles, (American Ceramic Society, Columbus, OH, 1984) pp. 94–104.

20. J. P. SMITH and G. L. MESSING, *J. Amer. Ceram. Soc.* **67** (1984) 238.
21. R. L. FULLMAN, *Trans. AIME* **197** (1953) 447.
22. J. D. BERNAL and J. MASON, *Nature* **188** (1960) 910.
23. G. D. SCOTT, *ibid.* **188** (1960) 908.
24. G. MASON, *ibid.* **217** (1968) 733.
25. J. L. FINNEY, *Proc. Roy. Soc. Lond. A* **319** (1970) 479.
26. D. J. ADAMS and N. A. MATHESON, *J. Chem. Phys.* **56** (1972) 1989.
27. A. J. MATHESON, *J. Phys. C. Solid State Phys.* **7** (1974) 2569.
28. H. J. FROST and R. RAJ, *J. Amer. Ceram. Soc.* **65** (1982) C-19.

Received 2 September 1991
and accepted 7 May 1992